



Rapid hydrogen production from water using aluminum nanoclusters: A quantum molecular dynamics simulation study



Priya Vashishta^{a,b,c,d,*}, Fuyuki Shimojo^{a,b,c,d,e}, Satoshi Ohmura^{a,b,c,d,e,f}, Kohei Shimamura^{a,b,c,d,e,g},
Weiwei Mou^{a,b,c,d}, Rajiv K. Kalia^{a,b,c,d}, Aiichiro Nakano^{a,b,c,d}

^a Collaboratory for Advanced Computing and Simulations, University of Southern California, Los Angeles, CA 90089-0242, USA

^b Department of Chemical Engineering & Materials Science, University of Southern California, Los Angeles, CA 90089-0242, USA

^c Department of Physics & Astronomy, University of Southern California, Los Angeles, CA 90089-0242, USA

^d Department of Computer Science, University of Southern California, Los Angeles, CA 90089-0242, USA

^e Department of Physics, Kumamoto University, Kumamoto 860-8555, Japan

^f Department of Physics, Kyoto University, Kyoto 606-8502, Japan

^g Department of Applied Quantum Physics and Nuclear Engineering, Kyushu University, Fukuoka 819-0395, Japan

ARTICLE INFO

Article history:

Received 15 July 2013

Received in revised form 2 December 2013

Accepted 9 December 2013

Available online 31 December 2013

Keywords:

Hydrogen production

Water

Aluminum nanoclusters

Quantum molecular dynamics simulation

ABSTRACT

It is hoped that a hydrogen-on-demand generator may one day start with just the turn of an ignition key, if the reaction kinetics is accelerated for the production of hydrogen gas from water. Our quantum molecular dynamics simulations have revealed the atomistic mechanism of rapid hydrogen production from water using aluminum nanoclusters, Al_n ($n = 16, 17$, and 18). We have found a low activation-barrier mechanism of hydrogen production, in which a pair of Lewis acid and base sites on the nanocluster surface plays a crucial role. Hydrogen production is assisted by rapid proton transport in water via a chain of hydrogen-bond switching events similar to the Grothuss mechanism. The solvation shell has been shown to greatly reduce the energy barrier. We have also found that the reaction rate does not depend strongly on the cluster size n , in contrast to the existence of magic numbers in gas-phase reaction. This work paves a way for a rational design of hydrogen-on-demand technologies.

© 2013 Elsevier B.V. All rights reserved.

1. Introduction

Metal carriers such as aluminum (Al) can be used in renewable energy cycles [1,2]. Here, exothermic reactions between metal and water produce hydrogen gas, followed by the endothermic reduction of metal-oxide products to regenerate metal fuel assisted by solar energy. One potential application of this technology is on-board hydrogen production for hydrogen-powered vehicles, but conventional metal–water reaction kinetics is too slow to make it commercially viable [3]. Previous experimental and theoretical works [4,5] showed the remarkable reactivity of superatoms [4,6] (i.e., clusters consisting of a magic number of Al atoms) with water in the gas phase. A remarkable size-selectivity was found for the reactivity of Al clusters with water, where an anion of Al cluster, Al_n^- (for instance, $n = 12$ or 17), reacts strongly with water molecules. How the reactivity of these Al “superatoms” [4,6] changes in bulk water is of great interest both scientifically and technologically. In addition, there are two unsolved questions: (1) what is the role of a solvation shell of water molecules that surrounds the Al nanocluster; and (2) whether the high size-selectivity observed in gas-phase Al_n^- -water reaction persists in liquid phase?

* Corresponding author at: Collaboratory for Advanced Computing and Simulations, University of Southern California, Los Angeles, CA 90089-0242, USA.

2. Simulation methods

In our quantum molecular dynamics (QMD) simulations [7–9], the electronic states are calculated using the projector-augmented-wave method [10], which is an all-electron electronic-structure-calculation method within the frozen-core approximation. In the framework of density functional theory (DFT), the generalized gradient approximation [11] is used for the exchange-correlation energy with non-linear core corrections [12]. The momentum-space formalism is utilized, where the plane-wave cutoff energies are 30 and 250 Ry for the electronic pseudo-wave functions and the pseudo-charge density, respectively. The energy functional is minimized iteratively using a preconditioned conjugate-gradient method. Projector functions are generated for the 3s, 3p and 3d states of Al, the 2s and 2p states of O, and the 1s state of H. The electronic-structure-calculation code has been implemented on parallel computers [13] by a hybrid approach combining spatial decomposition [14,15] (i.e., distributing real-space or reciprocal-space grid points among processors) and band decomposition (i.e., assigning the calculations of different Kohn–Sham orbitals to different processors). The program has been implemented using the message passing interface library for interprocessor communications. QMD simulations are carried out at a temperature of 1000 K in the canonical ensemble. The equations of motion are integrated numerically

with a time step of 11 a.u. (~ 0.264 fs). The system studied in our MD simulations consists of an Al_n ($n = 16, 17$, or 18) cluster and 84 H_2O molecules in a box of dimensions $12.58 \times 12.58 \times 18.87 \text{ \AA}^3$; see Fig. 1(a). The system size is determined from the density of water in the ambient condition, and periodic boundary conditions are imposed. The Γ point is used for Brillouin zone sampling.

3. Results

Fig. 1(b) shows the time evolution of the number of H–H bonds during the QMD simulations. We find rapid production of H_2 molecules in all cases, i.e., for Al_n with $n = 16, 17$, and 18 . Within 20 ps, three H_2 molecules are produced each in the Al_{16} and Al_{17} systems and six H_2 molecules are produced in the Al_{18} system. In the gas phase, the reactivity of Al_{17} with water molecules is much higher than that of Al_{16} and Al_{18} [4,5]. However, such size selectivity is absent in liquid phase.

Detailed analyses of simulation trajectories reveal a three-step process of H_2 production. An Al_n surface has sites with Lewis-acid character and those with Lewis-base character [4,5]. The reaction begins with the dissociation of an H_2O molecule bonding to an Al atom that has a Lewis-acid character [7–9], as one of its hydrogen atoms moves toward a neighboring H_2O molecule to form a hydronium ion (H_3O^+); see Fig. 2(a) for the case of Al_{17} . This is followed by a chain of hydrogen bond switching events, and finally a hydrogen atom bonds to another Al atom with Lewis-base character [7–9]. This proton transfer is thus induced by the complementary Lewis acid–base characters of the participating Al atoms.

To estimate the energy barrier for this water-dissociation process, we use the nudged elastic band (NEB) method to calculate the energy

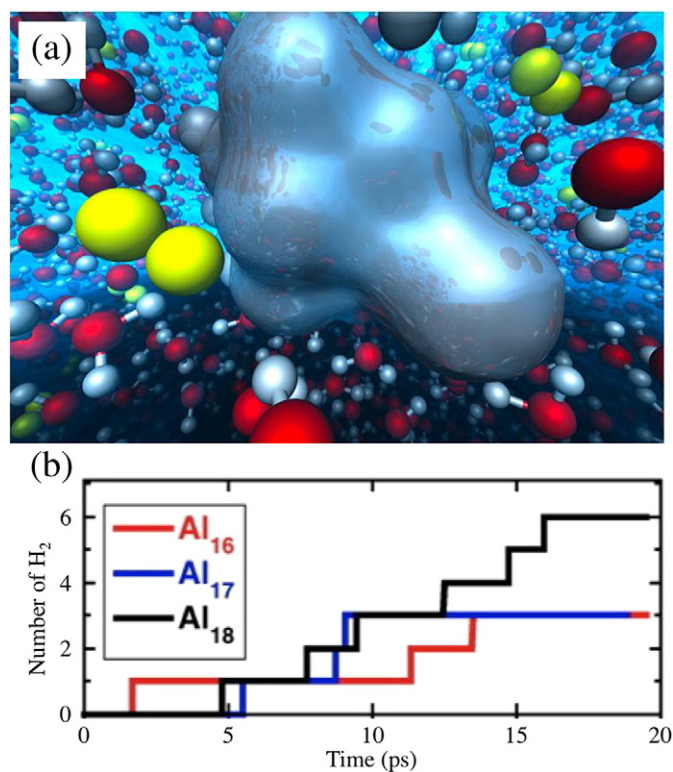


Fig. 1. (a) An aluminum nanocluster (colored silver in the center) producing hydrogen molecules (yellow) from water, where gray and red spheres are hydrogen and oxygen atoms, respectively. (b) The number of H–H bonds as a function of time for Al_n ($n = 16, 17$, and 18).

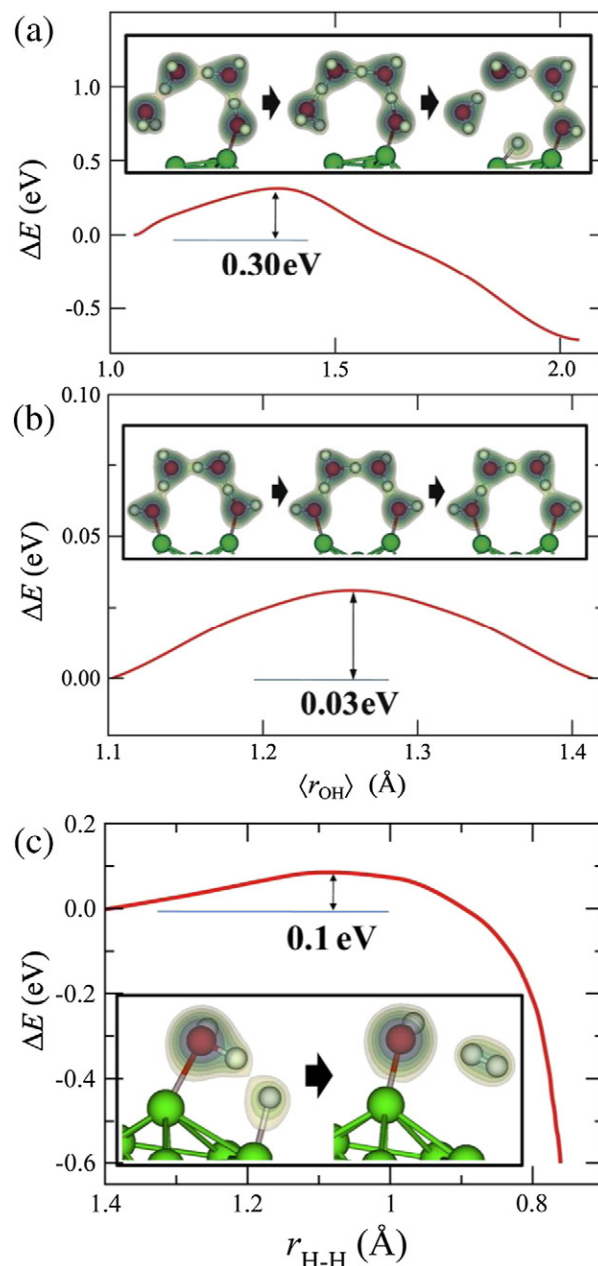
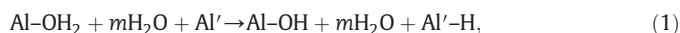


Fig. 2. Hydrogen production pathways in Al_{17} . (a) Energy profile along the reaction path for the production of a hydroxide ion and a hydrogen atom, $\text{Al} + 4\text{H}_2\text{O} + \text{Al} \rightarrow \text{Al}-\text{OH} + 3\text{H}_2\text{O} + \text{Al}-\text{H}$, obtained by NEB calculation. (b) Energy profile along the reaction, $\text{Al}-\text{OH} + 2\text{H}_2\text{O} + \text{Al}-\text{OH}_2 \rightarrow \text{Al}-\text{OH}_2 + 2\text{H}_2\text{O} + \text{Al}-\text{OH}$. Here, $\langle r_{\text{OH}} \rangle$ is the average length of the OH bond, which is broken in the reaction. (c) Energy profile along the reaction path of molecular hydrogen production, $\text{Al}-\text{OH}_2 + \text{Al}-\text{H} \rightarrow \text{Al}-\text{OH} + \text{Al} + \text{H}_2$, as a function of the distance between the two hydrogen atoms that form a hydrogen molecule. White, red and green spheres represent H, O and Al atoms, respectively. The distribution of the electron density larger than 0.05 a.u. is shown by contour surfaces.

profile along the reaction path for the production of a hydroxide group and a hydrogen atom on the Al cluster [7–9]:



where $m = 3$ for the process shown in Fig. 2(a). In Eq. (1), Al and Al' denote the Al atoms with Lewis acid and base characters, respectively, involved in the reaction. For $m = 3$, the activation energy is estimated to be $\Delta = 0.30 \text{ eV}$. The lowest energy barrier is $\Delta = 0.20 \text{ eV}$ for the case of $m = 1$. From the calculated values, the energy barrier for

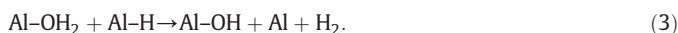
Eq. (1) is estimated to be $\Delta = 0.15 + 0.05 m$ eV for $m \geq 1$. The rates of these reactions at room temperature ($T = 300$ K) are estimated to be $k_1 = (k_B T/h) \exp(-\Delta/k_B T) \approx 10^7$ – 10^9 s⁻¹ according to the transition state theory, where k_B is the Boltzmann constant and h is the Planck constant.

The Al–OH product of Eq. (1) is often quickly converted back to Al–H₂O again by the Grotthuss mechanism, which involves a third Al atom (denoted as Al'') with an adsorbed water molecule:



Fig. 2(b) shows the energy profile for the reaction of Eq. (2) for $m = 2$ for Al₁₇. The activation energy of this reaction is estimated to be 0.10, 0.03, and 0.04 eV for $m = 1, 2,$ and $3,$ respectively. The corresponding rate is $k_2 = 10^{11}$ – 10^{12} s⁻¹ $\gg k_1$ at 300 K [7–9].

The final hydrogen-production reaction is expressed as



Namely, a hydrogen molecule is produced from H₂O adsorbed at a Lewis-acid site and H adsorbed at a neighboring Lewis-base site; see Fig. 2(c) for the case of Al₁₇ [7–9]. The corresponding activation energy is estimated to be $\Delta = 0.1$ eV. We also study the finite-temperature χ effect by calculating the activation free energy using thermodynamic integration, which gives a nearly identical value, $\Delta = 0.08$ eV, at 300 K [7–9]. The corresponding reaction rate is estimated as $k_{\text{H}_2} = (k_B T/h) \exp(-\Delta/k_B T) = 10^{11}$ s⁻¹ at room temperature.

To quantify the effect of the surrounding water molecules (i.e., solvation shell) on the energy barrier for H₂ production, we next consider the

same H₂-production mechanism as in Fig. 2(c) but by adding a surrounding water molecule; see H₄–O₂–H₅ in Fig. 3(a) for the case of Al₁₈. The extra water H₄–O₂–H₅ serves as a proton donor to form a branching hydrogen bond O₂–H₄···O₁. We perform NEB calculation to obtain the energy barrier as a function of $R_{\text{O}_1\text{-H}_4}$ as shown in Fig. 3(b). The energy barrier is reduced to below 0.02 eV (the blue dashed line) when $R_{\text{O}_1\text{-H}_4}$ is 1.75–2.0 Å, and the barrier increases to 0.08 eV for $R_{\text{O}_1\text{-H}_4} = 2.1$ Å. The red dashed line shows the limit, $R_{\text{O}_1\text{-H}_4} \rightarrow \infty$, in the absence of a solvation shell. This result indicates a significant role of solvation in greatly reducing the energy barrier of hydrogen production, thereby increasing the reaction rate.

It should be noted that our QMD simulations were performed with a constant simulation volume, so that the systems at higher temperatures are pressurized. This likely affects the number of produced H₂ molecules shown in Fig. 1. However, these simulations were performed simply to discover reaction events, and for all the discovered events, the corresponding reaction rates were estimated by NEB calculations on isolated clusters (see Figs. 2 and 3). The calculated reaction rates are thus free from the pressure problem.

4. Conclusion

Our QMD simulations have revealed the key design feature for low activation barriers for rapid H₂ production from water using Al nanoclusters, i.e., spatially proximate Lewis acid–base pairs. In a small nanocluster, local geometrical arrangement is not identical for all surface atoms. Consequently, some surface Al atoms act as Lewis acid and others as Lewis base. We have also found that hydrogen production is greatly assisted by rapid proton transport in water by a chain of hydrogen-bond switching events. This Grotthuss mechanism generates OH and H groups at Lewis acid and base sites, and converts OH groups back to water molecules.

Acknowledgments

This research was supported by the Department of Energy, Office of Science, Basic Energy Sciences, Materials Science and Engineering Division, Theoretical Condensed Matter Physics Program, Grant Number DE-FG02-04ER-46130. The simulations were performed at the Center for High Performance Computing and Communications of the University of Southern California.

References

- [1] A. Steinfeld, Sol. Energy 78 (2005) 603.
- [2] T. Yabe, S. Uchida, K. Ikuta, K. Yoshida, C. Baasandash, M.S. Mohamed, Y. Sakurai, Y. Ogata, M. Tuji, Y. Mori, Y. Satoh, T. Ohkubo, M. Murahara, A. Ikesue, M. Nakatsuka, T. Saiki, S. Motokoshi, C. Yamanaka, Appl. Phys. Lett. 89 (2006) 261107.
- [3] J. Petrovic, G. Thomas, Reaction of Aluminum With Water to Produce Hydrogen, U.S. Department of Energy, Washington, DC, USA, 2008.
- [4] P.J. Roach, W.H. Woodward, A.W. Castleman, A.C. Reber, S.N. Khanna, Science 323 (2009) 492.
- [5] A.C. Reber, S.N. Khanna, P.J. Roach, W.H. Woodward, A.W. Castleman, J. Phys. Chem. A 114 (2010) 6071.
- [6] D.E. Bergeron, A.W. Castleman, T. Morisato, S.N. Khanna, Science 304 (2004) 84.
- [7] F. Shimojo, S. Ohmura, R.K. Kalia, A. Nakano, P. Vashishta, Phys. Rev. Lett. 104 (2010) 126102.
- [8] S. Ohmura, F. Shimojo, R.K. Kalia, M. Kunaseth, A. Nakano, P. Vashishta, J. Chem. Phys. 134 (2011) 244702.
- [9] W. Mou, S. Ohmura, A. Hemeryck, F. Shimojo, R.K. Kalia, A. Nakano, P. Vashishta, AIP Adv. 1 (2011) 042149.
- [10] P.E. Blochl, Phys. Rev. B 50 (1994) 17953.
- [11] J.P. Perdew, K. Burke, M. Ernzerhof, Phys. Rev. Lett. 77 (1996) 3865.
- [12] S.G. Louie, S. Froyen, M.L. Cohen, Phys. Rev. B 26 (1982) 1738.
- [13] F. Shimojo, R.K. Kalia, A. Nakano, P. Vashishta, Comput. Phys. Commun. 140 (2001) 303.
- [14] A. Nakano, R.K. Kalia, K. Nomura, A. Sharma, P. Vashishta, F. Shimojo, A.C.T. van Duin, W.A. Goddard, R. Biswas, D. Srivastava, L.H. Yang, Int. J. High Perform. Comput. Appl. 22 (2008) 113.
- [15] K. Nomura, H. Dursun, R. Seymour, W. Wang, R.K. Kalia, A. Nakano, P. Vashishta, F. Shimojo, L.H. Yang, Proceedings of the International Parallel and Distributed Processing Symposium, IEEE, Washington, DC, USA, 2009.

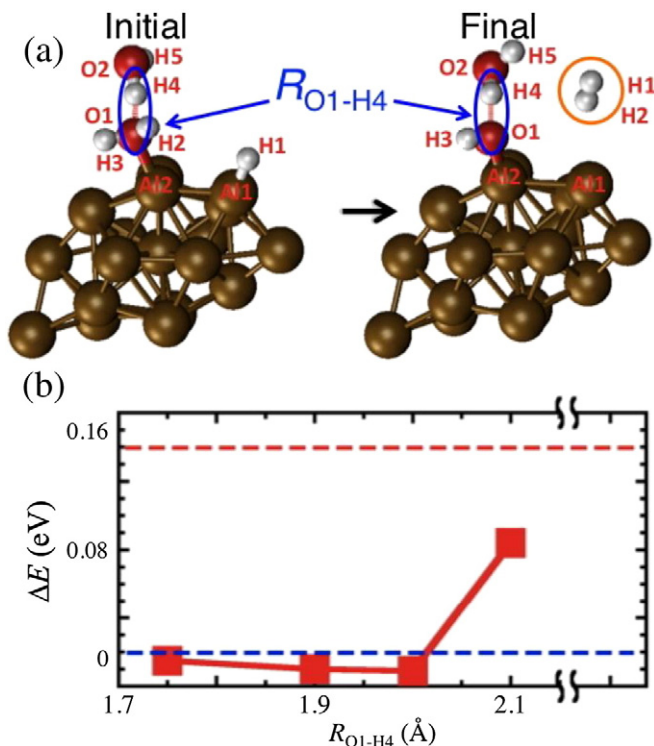


Fig. 3. (a) Initial and final states for H₂ production involving Al₁₈ in the presence of a surrounding water molecule H₄–O₂–H₅. Red, white and gold spheres represent O, H and Al atoms, respectively. The produced H₂ molecule is marked by the orange circle. (b) The reaction energy barrier for H₂ production for different constraint lengths $R_{\text{H}_4\text{-O}_1}$. The red dashed line is the asymptotic barrier of 0.14 eV for $r_{\text{H}_4\text{-O}_1} \rightarrow \infty$. The blue dashed line is at 0.02 eV.